

Fault Location in Power Transmission Lines using Autocorrelation Function

Danilo Pinto Moreira de Souza¹, Eliane da Silva Christo¹, Aryfrance Rocha Almeida², Kelly Alonso Costa³

¹Postgraduate Program in Computational Modeling in Science and Technology, Fluminense Federal University, BRAZIL
Email: danilopms@id.uff.br, elianechristo@id.uff.br

²Electrical Engineering, Federal University of Piauí, BRAZIL
Email: aryfrance@ufpi.edu.br

³Postgraduate Program in Production Engineering, Fluminense Federal University, BRAZIL
Email: kellyalonso@id.uff.br

Abstract—An electrical power system is subject to constant adversities due to its complexity, sensitivity and physical dimensions. Special emphasis is given to transmission lines (TL) that are the most vulnerable elements of an electrical system. Although most of the occurrences of distortions in the voltage signals from atmospheric discharges and overload are not detrimental to the energy supply, it is important to have control of these currents, since this allows the classification of the fault type and its geometric location on the transmission line. This study aims to compare different fault situations in a transmission line and to verify changes in time series models (TS). This study was carried out through computational tests performed with MatLAB® and RStudio® software. A total of 272 faults were simulated in different situations. The obtained results were compared with the Traveling Wave Theory (TWT), another quite widespread fault localization technique. The above study revealed the applicability of time series in oscillographic data of fault situations in transmission lines with errors lower than 1.25%.

Keywords—time series, line transmission, fault location, autocorrelation function (acf).

I. INTRODUCTION

With the importance of having an electrical system where continuity, compliance, flexibility and ease of maintenance are observed and guaranteed, the improvement and innovation of the techniques used in equipment for the protection and supervision of the system, as well as the expansion of the electric sector [1].

The precise location of faults assists the operating sector of the electrical system, reducing the time of occurrence of the disturbance, locating areas where faults occur regularly, reducing the occurrence of faults and minimizing the time of power failure. With this,

contributing to the continuity of the electric power supply [2][3][4][5].

There are many existing techniques to deal with the fault localization problem in transmission lines (TL). The classification of these techniques can be enhanced according to the number of terminals monitored in the TL. The use of data from more than one monitoring terminal involves online communication between them and use global positioning system (GPS), which increases the financial cost in the monitoring system. In [6], for example, it is monitor the fault current in three terminals of continuous transmission of high-voltage line. The use of single-terminal data eliminates the need for such investments.

Another way of classifying fault localization techniques is the way of analyzing the data. Most methods are based on the fundamental components of voltage and current sine [3]. In [7], for example, it provides an efficient algorithm with detection and fault isolation functions through a differential phase hopping pilot scheme to detect faulted branches in distribution networks. The method uses fundamental frequency components. In [8] is also used in fundamental frequency analysis in unbalanced three-phase faults observing the presence of negative sequence currents. Another example of fundamental frequency voltage signal analysis is presented in [9], which shows the behavior of the voltage drops for different fault situations in several scenarios of simulated sub transmission lines.

Another form of data processing is considering the high frequency components from the occurrence of the fault. However, in reality, immediately after the occurrence of a fault, transient displacement phenomena distort the steady state current and voltage waveforms. Consequently, these unwanted transient signal components must be eliminated before evaluating the voltage and current waveforms [10].

There are also methods that use computational intelligence through artificial neural networks (ANNs). An example of this application is shown in [11], which presents a new and accurate fault finding algorithm in a combined transmission line with underground power cable using the Adaptive Network Based Fuzzy Inference System (ANFIS).

The objective of this work is to present a fault localization technique in aerial transmission lines. The proposed method is based on the analysis of time series with autocorrelation functions, being the seasonality obtained for a failure situation, related to the location of this fault in the transmission line. The analysis of autocorrelation functions is used, for example, in cite parent, which addresses the uniformity property of the autocorrelation used to determine the delay time. This time

is a function of the position of the fault, employing numerical integration.

II. THEORY OF TRANSMISSION LINES DISTURBANCE

The transient voltage signals in a transmission line are oriented according to the Traveler Wave Theory (TWT) [12][13]. In this theory, the abrupt change of the voltage level in a transmission line propagates through this line from the point of origin of the perturbation to the ends of the line, in both directions. When finding a discontinuity in the "route" these waves are divided in reflected waves, and refracted waves. This process of reflection and refraction occurs several times, until the total absorption of the wave energy by the components of the line, reaching the steady state again [14]. Fig.1 shows the situation mentioned.

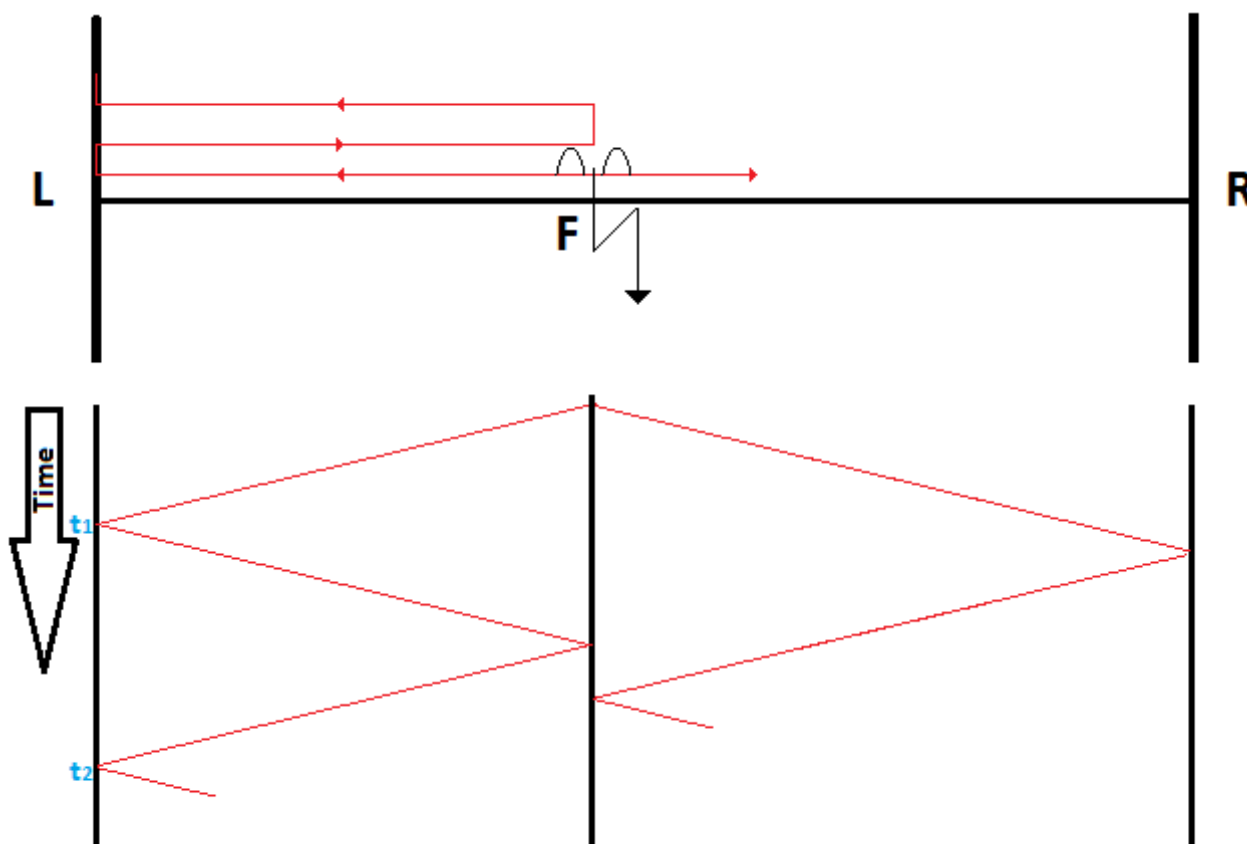


Fig. 1: Disturbance in the sinusoidal signals of phases A and B of TL. Beside, zoom in on the interest part in the analysis.

The behavior of the waves in the line depends on the intensity of the wave, the coefficients of refraction, reflection and damping and the speed of propagation. These in turn depend on the configuration of the transmission line, the fault resistance and, consequently, the type of fault. The angle of incidence of the disturbance in sinusoidal signals of the transmission line also influences the attenuation or expansion of the voltage peaks of the fault signals. In order for the TWT to be applicable and the results of the electromagnetic behavior

to be consistent with reality, it is necessary that the line model considered has its parameters distributed, for example the model JMARTI [15].

To determine the geographic location of the disturbance occurring at the point of transmission line are timed maximum points of the occurrences of times the monitored voltage (wave crests) at a terminal TL microarray [16]. These local maximum points on the voltage signals can be seen in Fig.2.

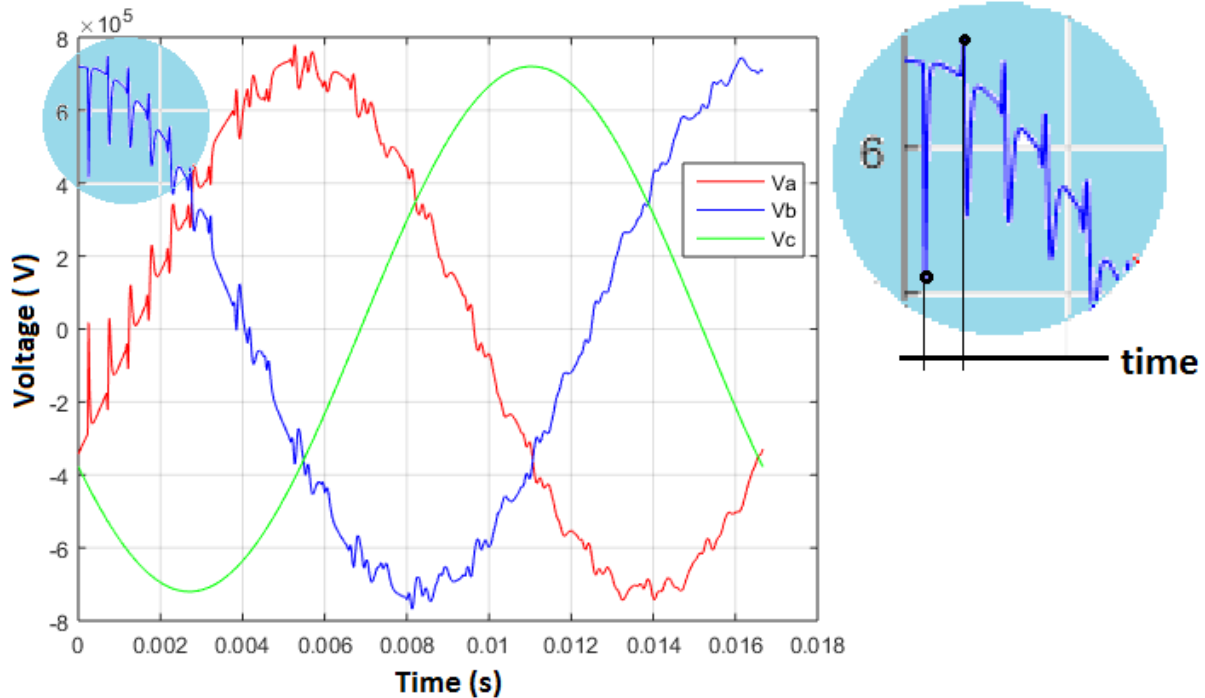


Fig. 2: Wave propagation in line transmission.

Once the times have been determined, the equation (1) is used to determine the fault distance.

$$d_{LF} = \frac{t_2 - t_1}{2} v \quad (1)$$

Where: d_{LF} is the distance between the monitoring terminal L and the point of occurrence of the fault F, t_1 is the time elapsing between the start of the timing and the arrival of the first wave front to the monitoring terminal, t_2 is the elapsed time between the start of the timing and the arrival of the second wavefront to the monitoring terminal, $v = \frac{1}{\sqrt{LC}}$ is the velocity of propagation of the wave in the line (approximated by the velocity of waves in a vacuum; l is the characteristic inductance of the circuit; c is the characteristic capacitance of the circuit). To compare the results obtained through the method proposed in this work, equation (1) is used.

III. THE PROPOSED METHOD

In order to extract distance from only one monitor terminal, it is necessary to observe the pattern generated by the wave propagating between the fault point and the monitoring point. The periodicity of the analyzed signal is due to its constant rate of propagation. Also, the instants referring to the points of maximum locations characterize the moments at which the wave front reaches the

monitoring terminal. Thus, calculating the time interval between two consecutive maxima is the equivalent of determining the propagation time of the wave between the fault point and the monitoring point.

It is initially investigated the presence of trends and seasonality in the time series to be investigated [17][18][19][20]. The trend of a series indicates its "long-term" behavior, that is, whether it grows, decreases, or remains stable, and how fast these changes are. Regarding the trend, the Cox-Stuart test is used[21]. As the series shows symmetry with respect to the vertical axis, initially the temporal series is divided into two parts. Thus the two series obtained do not present symmetry. Since this symmetry makes it impossible to use the Cox-Stuart Test, it makes erroneous values. Once the test was performed, it indicated that the series had a 87% chance of showing a tendency. It was also observed that this tendency is due to the sinusoid coming from the nominal frequency of the transmission line. To determine the trend, the Fourier series analysis is used. The Fig.3 (a) shows the calculated trend and the original series. The Fig.3 (b) shows the time series without the presence of trend. The series of trends previously calculated by Fourier series [17][18][19][20][22] was extracted from the original time series.

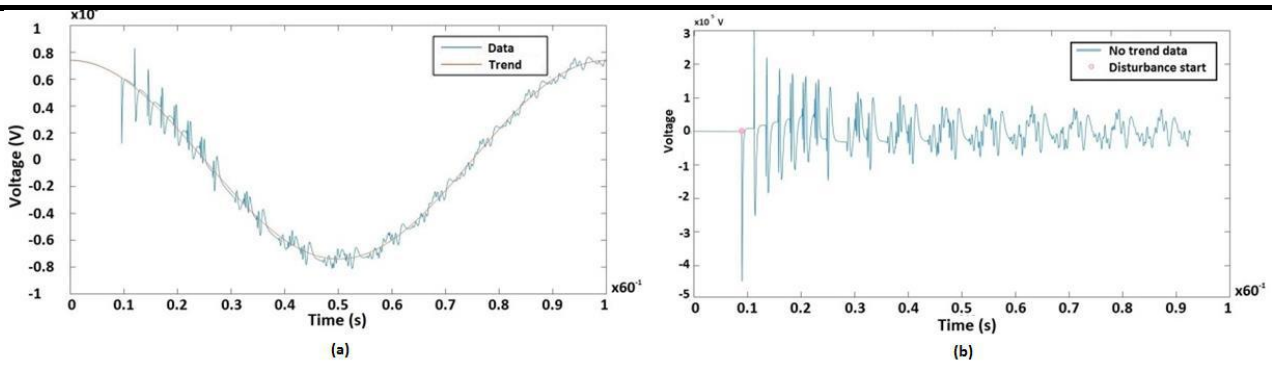


Fig. 3: (a) Graph with time series and their respective trend. (b) Decoupled voltage signal. The starting point of the disturbance is related to the incidence angle of the fault on the transmission line.

From the new time series generated it is possible to monitor the differences between the consecutive voltage values. This makes it possible to terminate the onset of the disturbance at the fundamental voltage signal (60 Hz), thereby determining the incidence angle of the fault. The next step is to eliminate the pre-fault voltage data (before the onset of the disturbance), considering only the post-fault data. The procedures described in this paragraph are related to what is called “Algorithm 1” in Fig. 5. Thus, this algorithm is able to determine both the transmission line phases that are involved in the fault, as well as to determine the angle of incidence of this fault in the line.

For the determination of seasonality, the analysis was used the auto correlation function [10][15]. Autocorrelation consists of the cross-correlation of a signal with itself. Used to find patterns of repetition or obscured by noises.

The next step is to calculate the autocorrelation function of the new time series without trends and with

post-fault data. Once this calculation has been made, to determine the seasonality value, an arithmetic mean between the positions of the lags with the highest local values is made. This obtained value is taken as being the seasonality for the fault situation analyzed. Once this procedure has been performed several times, there will be several seasonal values close to the same fault distance. Again, the arithmetic mean of these seasonal values is calculated, and there will be only one seasonal value attached to a missing distance. The procedures described in this paragraph consist of what is called “Algorithm 2” in Fig. 5.

Fig. 4 (a) shows the graph of the autocorrelation function with 200 lags for a random fault situation contained in Table 1. For all cases the behavior is similar, with the characteristic that the larger the occurrence distance of the larger fault the distance between the maximum local lags. The existing pattern of repetition and damping is observed. In Fig. 4 (b) there is a zoom for the first 18 lags of the illustration at the side.

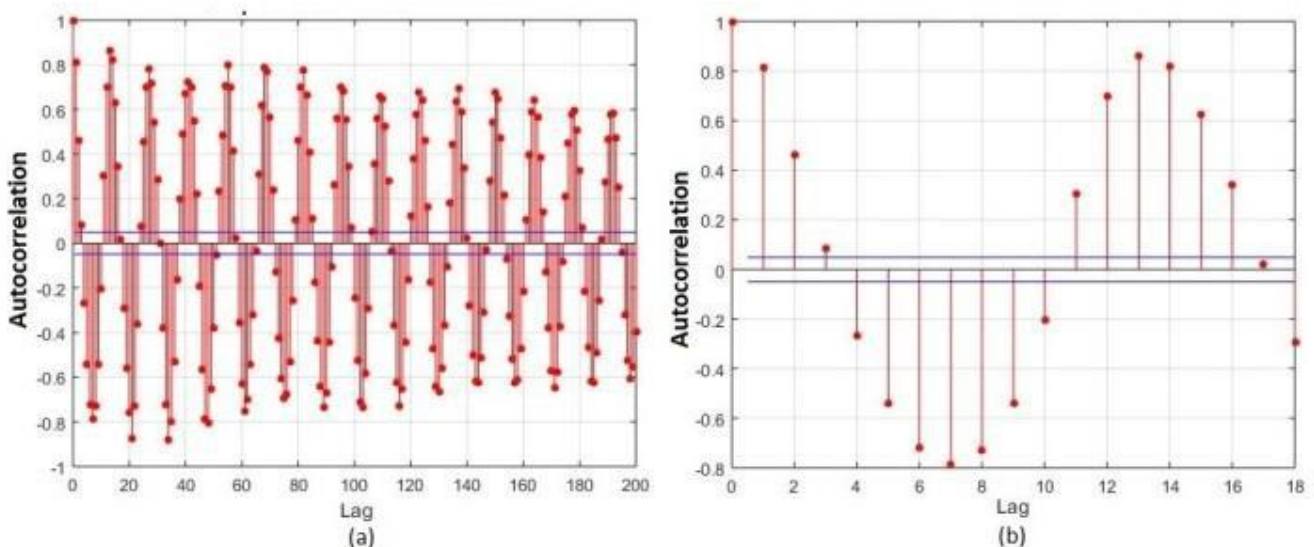


Fig. 4: Sample of the autocorrelation function (acf).

With the mean seasonality information for each distance value it is possible to calculate an adjustment curve relating the two terms. This can be done by using the method of least squares (MLS)[12]. The generation of a polynomial relating seasonality to distance allows the estimation for several fault situations only with the information of the value of seasonality. All steps

described above are illustrated in Fig.5 below. It is observed the existence of two steps to be followed: the first is the determination of the polynomial seasonality versus distance that applies to all occurrence of fault in the modeled transmission line; the second step consists in the use of this polynomial to determine the existence of fault as well as its location in the transmission line.

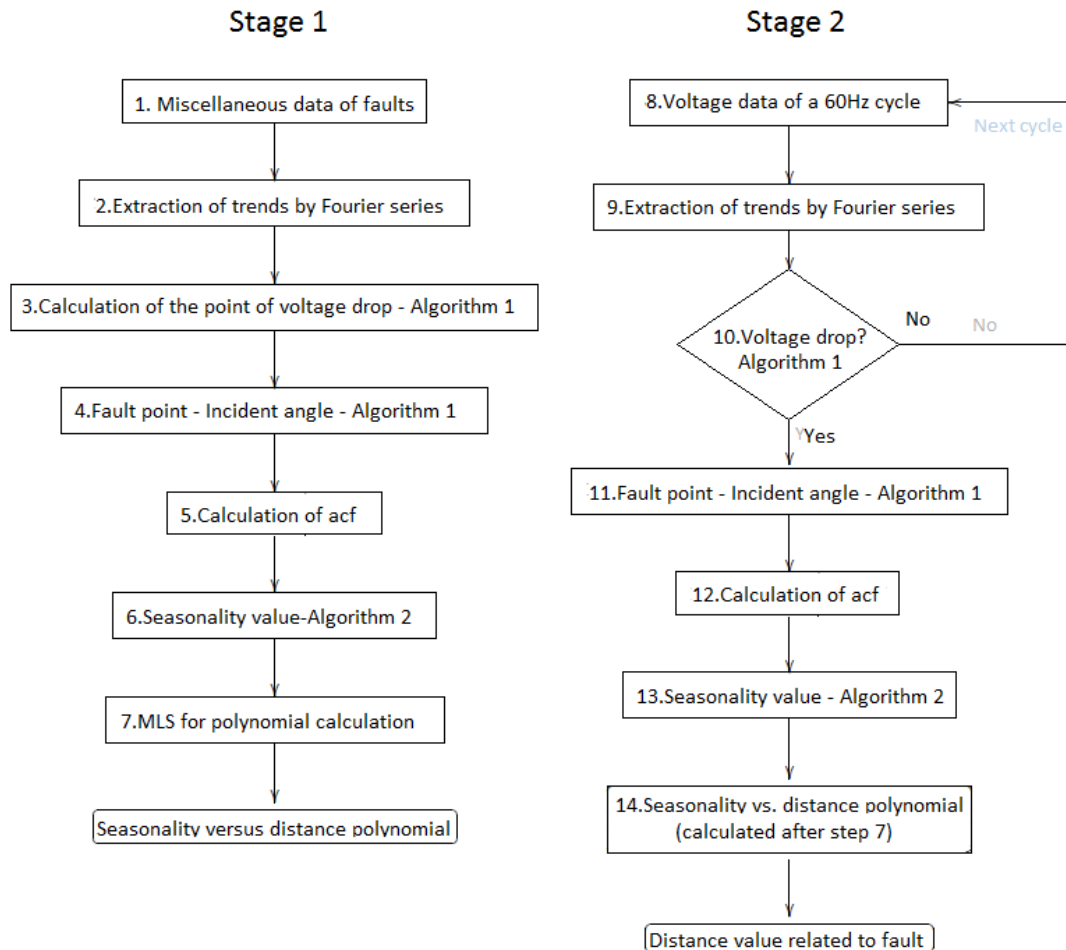


Fig.5: Flowchart.

IV. SIMULATION RESULT

In the ATP draw® software [23], fault simulations were performed on a three-phase aerial transmission line of 500kV, 60Hz and 200km extension. The model of line used in the modeling is the model JMARTI [15], well indicated for study of transient signals. The input parameters for the simulations are the simulation time, the

sampling frequency of the relay, the fault location on the line, as well as the elements involved. In addition, the angle of incidence of the fault in the line, which consists of the closing contact between the phases and the earth involved. For faults with the earth, the value of the ground resistance is also the input parameter.

Table.1: Simulation settings made.

Involved Elements	Fault Distance(m)	Angle of Incidence(°)	Sampling Frequency (kHz)	Number of Simulation
A-B	5:5:30 ; 40:10:100 ; 120 : 20 : 180 ; 190	0 : 30 : 330	100 kHz	216
A-B	5 10 2045 7084 155	0 : 45 : 315	200 kHz	56
Total of simulations				272

The least squares method (MLS)[1] is used to determine the relationship between seasonality and distance. Initially, a mean is performed between seasonality values related to the same distance value and different values of fault incidence angles. As a result, there is a single value of seasonality related to each distance. The equation (2) shows the result obtained for the biphasic fault data at 100kHz (Table 1).

$$y = 4.2 \times 10^{-8}x^5 - 1.4 \times 10^{-5}x^4 + 1.6 \times 10^{-3}x^3 - 7.7 \times 10^{-2}x^2 + 2.9x - 12.6 \quad (2)$$

Where x denoted the seasonality and y the distance. The values of x are taken from the seasonal means for each distance value (example for one of the values of x in Table 2).

Plotting the graphs from the equation (2) and the mean seasonality versus distance data, results in the Fig.6. This adjustment curve gives an average relative error of 2.84% and Pearson's correlation coefficient of 1.00, indicating that distance and seasonality are strongly correlated.

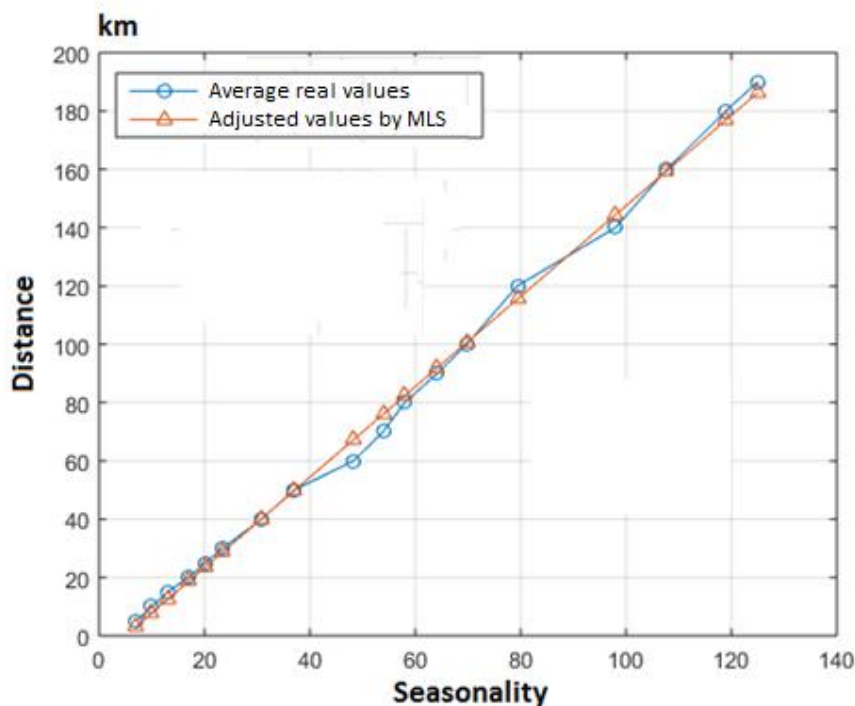


Fig.6: Seasonality Vs. Distance and Adjustment by M

Table 2 shows an example for the distance of 5 km. This table shows the values calculated for the angles as well as their respective errors and the results of

the calculated distances and the errors made. It is also possible to visualize (last two columns) the distances and relative errors of the moving waves.

Table 2: Biphasic fault between A–B phases, distance 45km and sample frequency of 100kHz. Calculation of incidence angles and calculation of fault distance by: ¹MLS method, ²TWT method. *Average seasonality for 45km.

Fault Number (n)	Angle (°)	Calculated Angle (°)	Relative Error(%) equation (4)	Seasonality (acf)	Distance (km) ¹	Relative Error ¹ (%) equation (5)	Distance (km) ²	Relative Error ² (%) equation (5)
1	0	3.13	3.13	66	45.14	0.07	44.98	0.01
2	45	48.58	7.95	66	45.14	0.07	44.98	0.01
3	90	93.91	4.35	66	45.14	0.07	43.48	0.76
4	135	139.25	3.15	66	45.14	0.07	43.48	0.76
5	180	182.43	1.35	66	45.14	0.07	43.48	0.76
6	225	227.77	1.23	66	45.14	0.07	44.98	0.01
7	270	273.10	1.15	66	45.14	0.07	44.98	0.01
8	315	318.44	1.09	65	45.14	0.07	44.98	0.01
Mean values(s = 8)	Mean values	equation (6) 2.92		65.88*	45.05	equation (6) 0.09	44.42	equation (6) 0.29

Plotting the graphs from the equation (3) and the mean seasonality versus distance data, results in the Fig.7. This adjustment curve gives an average relative error

of 0.51% and correlation coefficient of 1.00, indicating that distance and seasonality are strongly correlated.

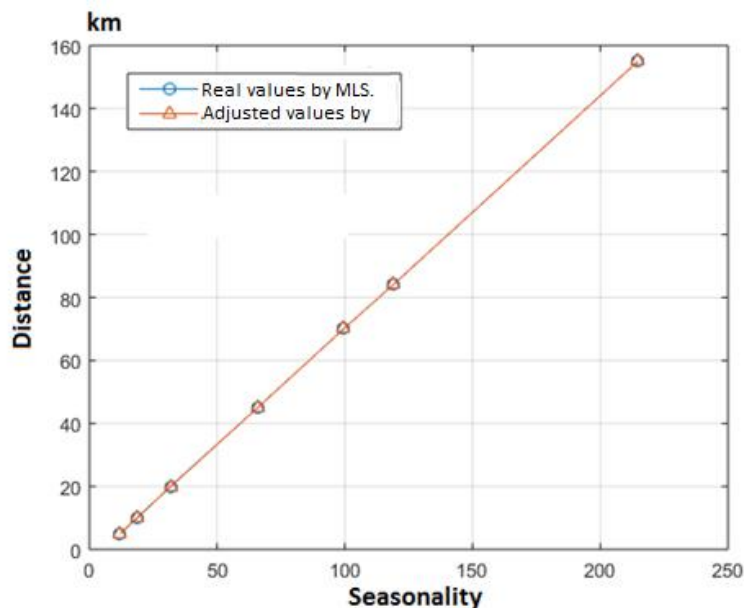


Fig.7: Seasonality Vs. Distance and Adjustment by MLS.

The same analysis is done for voltage data with a sampling frequency of 200kHz. The mean of the seasonal values for each fault distance is obtained, and using the MLS has the equation (3).

$$y = 6.5 \times 10^{-10}x^5 - 3.0 \times 10^{-7}x^4 + 4.9 \times 10^{-5}x^3 + 0.9x - 4.9 \quad (3)$$

Where x denoted the seasonality and y the distance. The

values of x are taken from the seasonal means for each distance value (example for one of the values of x in Table 3)

Table 3 shows the calculation and relative error for the incidence angles of the fault in the sinusoid of the transmission line and the calculation of distance and relative error for the same distance quoted. It is also possible to visualize (last two columns) distances and relative errors for the desire of the traveling waves.

Table.3: Biphasic fault between A–B phases, distance 40km and sample frequency of 200kHz. Calculation of incidence angles and calculation of fault distance by: ¹MLS method, ²TWT method. *Average seasonality for 40km.

Fault Number(n)	Angle (°)	Calculated Angle (°)	Relative Error (%) equation (4)	Seasonality (acf)	Distance (km) ¹	Relative Error ¹ (%) equation (5)	Distance (km) ²	Relative Error ² (%) equation (5)
1	0	2.59	2.59	31	39.16	0.42	38.97	0.52
2	30	32.81	9.35	30	37.90	1.05	38.97	0.52
3	60	63.02	5.04	31	39.16	0.42	38.97	0.52
4	90	93.45	3.84	31	39.16	0.42	38.97	0.52
5	120	123.67	3.06	31	39.16	0.42	38.97	0.52
6	150	151.73	1.15	31	39.16	0.42	38.97	0.52
7	180	181.94	1.08	31	39.16	0.42	38.97	0.52
8	210	212.16	1.03	30	37.90	1.05	38.97	0.52
9	240	242.37	0.99	31	39.16	0.42	38.97	0.52
10	270	272.59	0.96	31	39.16	0.42	38.97	0.52
11	300	302.81	0.93	31	39.16	0.42	38.97	0.52
12	330	333.02	0.91	30	37.90	1.05	38.97	0.52
Mean values(s = 12)	Mean values		equation (6) 2.58	30.75*	38.85	equation (6) 0.58	38.97	equation (6) 0.52

The errors shown in the previous tables are calculated according to the statements shown below. For the errors in the calculation of the values of the angles was used the equation (4). In this equation the real values and the calculated values are considered.

$$\text{error}_a^{(n)}(\%) = \frac{|a_r - a_c|}{a_r} \times 100 \quad (4)$$

Where: $n = (1, 2, \dots, s)$, error_a is the value of the error in the angle calculation given in percentage, a_r is the real value of the angle of incidence of fault, a_c is the calculated value of the angle of incidence of the fault, n is the fault situation, s is the number of simulations for the same fault characteristics except for the angle of incidence of the sinusoidal signal disturbance.

The error values for the distances were calculated according to the following equation (5) [14][23]:

$$\text{error}_d^{(n)}(\%) = \frac{|d_r - d_c|}{d_l} \times 100 \quad (5)$$

Where: $n = (1, 2, \dots, s)$, error_d is the value of the error in the distance calculation given in percentage, d_r is the real value of the occurrence of line fault, d_c is the calculated value of the fault occurring on the line, d_l is the total length of the transmission line (in this simulation $d_l = 200\text{km}$), s is the number of simulations for the same fault characteristics except for the angle of incidence of the sinusoidal signal disturbance.

And the mean errors were calculated according to equation (6):

$$\text{error}_m = \sum_{n=1}^s \frac{\text{error}^{(n)}}{s} \quad (6)$$

Where: error_m is the mean error for the same characteristics except for the angle of incidence, $\text{error}^{(n)}$ is the error previously calculated in equation (5) or equation (6).

V. CONCLUSION

This paper presents a new method of locating faults in high voltage aerial transmission lines based on the analysis of the autocorrelation function of the uniterminal voltage signal. A hypothetical line is implemented in the ATPdraw® software and different types of faults are simulated in the AC transmission system. Fault voltage signals are detected in only one terminal, which in practice results in cost savings, and a database is generated to allow the extraction of information about the locations of the simulated faults. Through the relationship between the seasonality in the time series and the location of the fault, a new localization algorithm is proposed. In practice, this location provides power utilities with statistical failure and agility maintenance.

When analyzing these time series, it is possible to understand changes in the behavior of the autocorrelation

functions, once the characteristics of the faults in the simulated line have changed. The main objective of this analysis is that only from the voltage oscillography can it be possible to calculate the geographical location of the occurrence of the fault in the line, as well as to classify the type of fault. The results obtained were satisfactory when compared to the results obtained by the theory of the traveling waves, considering the limitations for application of the method.

Currently the method is inapplicable to faults involving the earth component due to the appearance of the refracted waves, which totally modifies the pattern observed in other situations. This limitation can be solved with the pre-use of frequency bands.

In addition, because the acf lags are integers, this causes a seasonal value to correspond to a range containing several distance values. This restriction of the proposed method to identify small changes in distances is minimized as the frequency is increased. This reduces the range of distances mentioned in relation to the same seasonality detected in acf.

However, while increasing the frequency increases the sensitivity of the method, which means that the execution times of the algorithms are larger. Due to computational limitations, sample of relatively low frequencies were used: 100kHz and 200kHz. However with parallel programming, for example, this problem of execution speed can be solved.

In order to verify perception to frequency variations, it is possible to perform fault simulations considering distances close to each other, in order to determine which range of distances represents a single seasonal value.

The main contribution of this method lies in the innovation in the use of time series analysis in order to locate faults in transmission lines. Despite the necessary improvements mentioned above, it is seen that this method is comparable to the techniques already used in a practical way. Once the improvements have been made, greater accuracy in the fault location is expected.

For the development of future research, suggest the study of partial autocorrelation function (pacf) and spectral autocorrelation function (sacf). The pacf also highlights relevant data previously obscured by noise. The sacf brings with it a frequency analysis that proves to be quite effective for these types of data.

ACKNOWLEDGEMENTS

The authors acknowledge the financial support from CAPES.

REFERENCES

- [1] Costa, F. F., Formiga, D. A., Ferreira, R. R., Sousa, T., & Costa, F. B. (2013, June). A recursive least-

- squares aided by pre-filtering for phasor-estimation in distance protection. In PowerTech (POWERTECH), 2013 IEEE Grenoble (pp. 1-6). IEEE.
- [2] Agarwall, N., Mahela, O., & Kumar, B. (2016). Detection of power system faults in the presence of linear loads using stockwell transform. *Journal of Electrical and Electronics Engineering*, 2, 37-45.
- [3] Costa, F. B., Souza, B. A., & Brito, N. S. D. (2009, June). A wavelet-based method for detection and classification of single and crosscountry faults in transmission lines. In *International Conference on Power Systems Transients* (pp. 1-8).
- [4] Suresh, S., Nagarajan, R., Sakthivel, L., Logesh, V., Mohandass, C., & Tamilselvan, G. (2017). Transmission Line Fault Monitoring and Identification System by Using Internet of Things. *International Journal of Advanced Engineering Research and Science (IJAERS)*, 4, 9-14.
- [5] Robertson, D. C., Camps, O. I., Mayer, J. S., & Gish, W. B. (1996). Wavelets and electromagnetic power system transients. *IEEE Transactions on Power Delivery*, 11(2), 1050-1058.
- [6] Li, J., Yang, Q., Mu, H., Le Blond, S., & He, H. (2018). A new fault detection and fault location method for multi-terminal high voltage direct current of offshore wind farm. *Applied Energy*, 220, 13-20.
- [7] El Halabi, N., García-Gracia, M., Borroy, J., & Villa, J. L. (2011). Current phase comparison pilot scheme for distributed generation networks protection. *Applied Energy*, 88(12), 4563-4569.
- [8] Jia, K., Gu, C., Li, L., Xuan, Z., Bi, T., & Thomas, D. (2018). Sparse voltage amplitude measurement based fault location in large-scale photovoltaic power plants. *Applied Energy*, 211, 568-581.
- [9] Shankaraiah, R & Shankaraiah (2016). Analysis of Voltage Sag in Sub Transmission System. *International Journal of Advanced Engineering Research and Science (IJAERS)*, 3, 9-13
- [10] Paithankar, Y. G., & Sant, M. T. (1985). A new algorithm for relaying and fault location based on autocorrelation of travelling waves. *Electric Power Systems Research*, 8(2), 179-185.
- [11] Sadeh, J., & Afradi, H. (2009). A new and accurate fault location algorithm for combined transmission lines using adaptive network-based fuzzy inference system. *Electric Power Systems Research*, 79(11), 1538-1545.
- [12] Cavalcante, P. A., Trindade, F. C., & de Almeida, M. C. (2013). Transmission Lines Fault Location: A Mathematical Morphology-Based Approach. *Journal of Control, Automation and Electrical Systems*, 24(4), 470-480.
- [13] Prakasam, D. K., Suryakalavathi, D. M. & Reddy, M. R. (2015). Detection and location of faults in 11kv underground cable by using continuous wavelet transform (cwt). *Journal of Electrical and Electronics Engineering*, 10, 44-50.
- [14] Souza, T. B. P. (2007). *Análise de Ondas Viajantes em Linhas de Transmissão para Localização de Falhas: Abordagem via Transformada Wavelet* (Doctoral dissertation, Master's Thesis, Federal University of Pará (UFPA): Belém, Brazil, 2007. (In Portuguese)).
- [15] Marti, J. R. (1982). Accurate modelling of frequency-dependent transmission lines in electromagnetic transient simulations. *IEEE transactions on power apparatus and systems*, (1), 147-157.
- [16] Souza, S. C. A., Braga, A. P. S., Leão, R. P. S., Almeida, O. M. A., Almeida, A. R., & Abreu, F. C. M. *Uso de Redes Neurais Artificiais e Transformada de Stockwell na Localização de Falhas em Linhas de Transmissão*; Universidade Federal do Ceará (UFC): Fortaleza, Brazil, 2015. Google Scholar.
- [17] Crăciun, M., Vamoş, C., & Suci, N. (2018). Analysis and generation of groundwater concentration time series. *Advances in Water Resources*, 111, 20-30.
- [18] de Oliveira Silva, R., da Silva Christo, E., & Alonso Costa, K. (2014). Analysis of Residual Autocorrelation in Forecasting Energy Consumption through a Java Program. In *Advanced Materials Research* (Vol. 962, pp. 1753-1756). Trans Tech Publications.
- [19] de Jesus, J. C., da Silva Christo, E., da Silva Garcia, V., & Alvarez, G. B. (2016). Time Series Analysis For Modeling Of Glioma Growth In Response To Radiotherapy. *IEEE Latin America Transactions*, 14(3), 1532-1537.
- [20] Deb, C., Zhang, F., Yang, J., Lee, S. E., & Shah, K. W. (2017). A review on time series forecasting techniques for building energy consumption. *Renewable and Sustainable Energy Reviews*, 74, 902-924.
- [21] Cox, D. R., & Stuart, A. (1955). Some quick sign tests for trend in location and dispersion. *Biometrika*, 42(1/2), 80-95.
- [22] Pinto Moreira de Souza, D., da Silva Christo, E., & Rocha Almeida, A. (2017). Location of Faults in Power Transmission Lines Using the ARIMA Method. *Energies*, 10(10), 1596.
- [23] Cantanheda, S. S. T. (2011). *Localização de falhas em linhas de transmissão por meio de ondas viajantes* (Master's thesis, Federal University of Piauí).